

Electronic Supporting Information

Cationic PCP iridaepoxide and carbene complexes for facile water elimination and activation processes.

Lauren E. Doyle, Warren E. Piers,* David W. Bi

University of Calgary, Department of Chemistry, 2500 University Drive N.W., Calgary, Alberta, Canada, T2N 1N4.

Contents

General Considerations	S2
Figure S1. ^1H NMR spectra of the reaction of $\text{Me}_3\text{SiNTf}_2$ with 2-Cl .	S3
Figure S2. Variable temperature $^{31}\text{P}\{^1\text{H}\}$ NMR spectra (243 MHz) of 4-Cl .	S4
Figure S3. Molecular structure of 4-Cl .	S4
Figure S4. ^1H NMR spectrum of 4-OH in CD_2Cl_2 .	S5
Figure S5. ^1H NMR spectrum of 3-NTf₂ in CD_2Cl_2 .	S5
Figure S6. $^{31}\text{P}\{^1\text{H}\}$ and ^{19}F NMR spectra of 3-NTf₂ in CD_2Cl_2 .	S6
Figure S7. $^{13}\text{C}\{^1\text{H}\}$ NMR spectrum of 3-NTf₂ in CD_2Cl_2 .	S6
Figure S8. $^{31}\text{P}\{^1\text{H}\}$ NMR spectrum in of the reaction of 3-Cl , AgNTf_2 and excess water.	S7
Figure S9. ^1H NMR spectrum of 4-OPh in CD_2Cl_2 .	S7
Figure S10. $^{31}\text{P}\{^1\text{H}\}$ (left) and ^{19}F (right) NMR spectra of 4-OPh in CD_2Cl_2 .	S8
Figure S11. $^{13}\text{C}\{^1\text{H}\}$ NMR spectrum of 4-OPh in CD_2Cl_2 .	S8
Figure S12. ^1H NMR spectrum of 2-NTf₂ in CD_2Cl_2 .	S9
Figure S13. $^{31}\text{P}\{^1\text{H}\}$ and ^{19}F NMR spectra of 2-NTf₂ in CD_2Cl_2 .	S9
Figure S14. $^{13}\text{C}\{^1\text{H}\}$ NMR spectrum of 2-NTf₂ in CD_2Cl_2 .	S10
Figure S15. ^1H NMR spectrum of 3-OPh in CD_2Cl_2 .	S10
Figure S16. $^{13}\text{C}\{^1\text{H}\}$ NMR spectrum of 3-OPh in CD_2Cl_2 .	S11

Figure S17. ^1H NMR spectrum of 4-Cl in CD_2Cl_2 .	S11
Figure S18. $^{31}\text{P}\{^1\text{H}\}$ and ^{19}F NMR spectra of 4-Cl in CD_2Cl_2 .	S12
Figure S19. $^{13}\text{C}\{^1\text{H}\}$ NMR spectrum of 4-Cl in CD_2Cl_2 .	S12
Figure S20. $^{13}\text{C}\{^1\text{H}\}$ NMR spectrum of 4-OH in CD_2Cl_2 .	S13
Figure S21. ^1H NMR spectrum of 5 in CD_2Cl_2 .	S13
Figure S22. $^{13}\text{C}\{^1\text{H}\}$ NMR spectrum of 5 in CD_2Cl_2 .	S14
Figure S23. ^1H NMR spectrum of 6-acetone in acetone- d_6 .	S14
Figure S24. $^{13}\text{C}\{^1\text{H}\}$ NMR spectrum of 6-acetone in acetone- d_6 .	S15
Table S1. Data collection and structure refinement details.	S16

General Considerations. Storage and manipulation of all compounds were performed under an argon atmosphere either in a VAC glove box or using a double manifold high vacuum line using standard techniques. Pentane and hexanes were dried and purified using a Grubbs/Dow solvent purification system and stored in 500 mL thick-walled vessels over sodium/benzophenone ketal. Dichloromethane and dichloromethane- d_2 were dried over calcium hydride and vacuum transferred into thick-walled vessels for storage over activated sieves. Acetonitrile and acetone- d_6 were dried and stored over activated sieves. Bromobenzene- d_5 was dried and stored over sodium/benzophenone ketal. All dried solvents were degassed and vacuum distilled prior to use. ^1H and ^{13}C NMR chemical shifts were referenced to residual solvent protons and naturally abundant ^{13}C resonances for all deuterated solvents. Prior to acquisition all other spectra were referenced to external standards: ^{19}F (C_6F_6 in bromobenzene- d_5), ^{31}P (85% H_3PO_4 in D_2O). NMR spectra were processed and analyzed with MestReNova (v9.0.1-13254) NMR software. Chemical shift assignments are based on ^1H , $^{13}\text{C}\{^1\text{H}\}$, $^{31}\text{P}\{^1\text{H}\}$, ^{19}F , ^1H - ^1H -COSY, ^1H - ^{13}C -HSQC and ^1H - ^{13}C -HMBC NMR experiments performed on Bruker RDQ-400, Ascend-500 or Avance-600 spectrometers. Ultra High Purity Hydrogen was purchased from Praxair and used as received. Nitrous oxide (99%) was purchased from Sigma-Aldrich and used as received. All other reagents were purchased from Sigma-Aldrich and used as received. X-ray crystallographic analyses were performed on either a Nonius KappaCCD diffractometer or a Bruker Smart diffractometer equipped with Apex II detector. Samples were coated in Paratone 8277 oil

(Exxon) and mounted on a glass fibre. Full crystallography details can be found in independently uploaded .cif files. All Elemental analyses were obtained by the Instrumentation Facility of the Department of Chemistry, University of Calgary. Solution high resolution-mass spectrometry experiments were performed on a Kratos MS-80 spectrometer (direct ESI-MS or APCI-MS) on samples prepared in the glove box in a gas tight syringe.

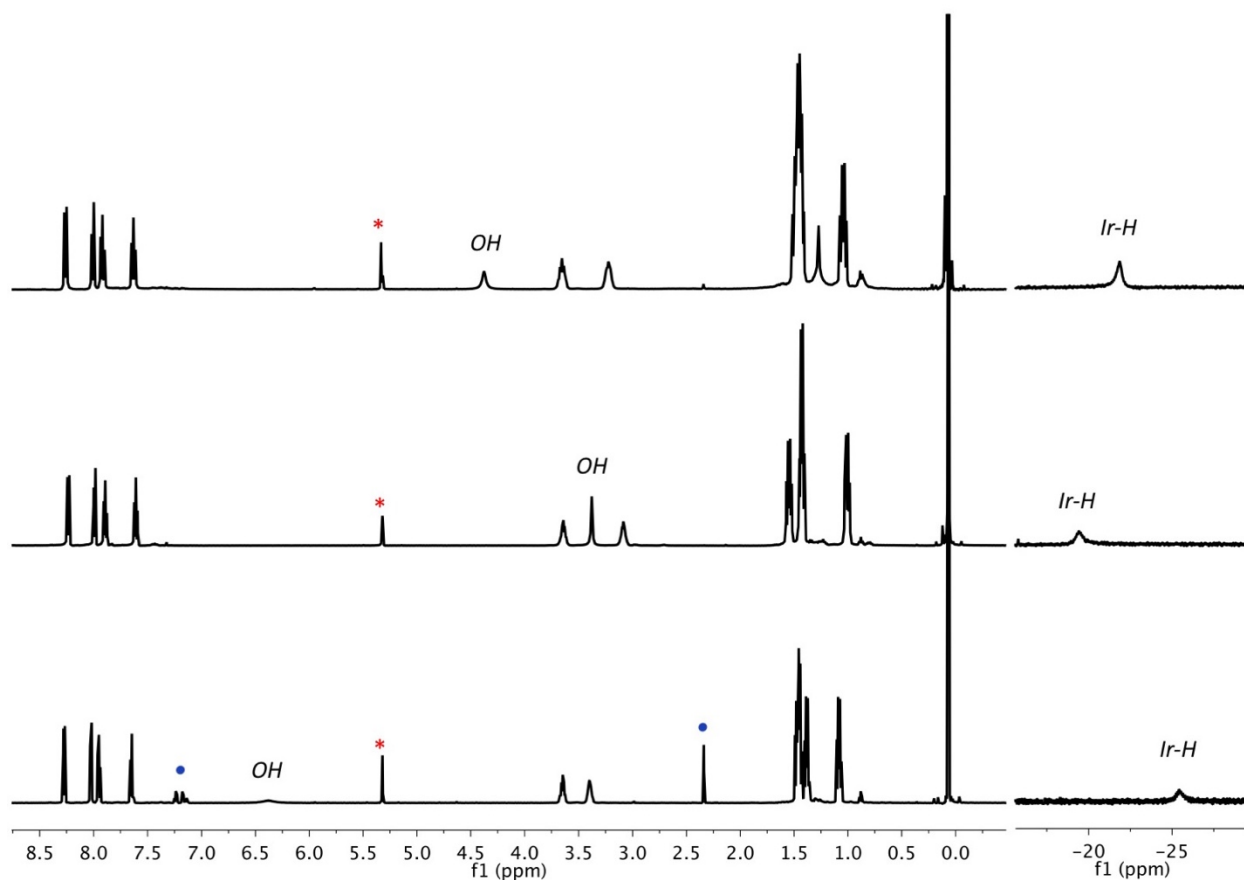


Figure S1. Three different room temperature *in situ* ^1H NMR spectra (500 MHz) of the reaction of $\text{Me}_3\text{SiNTf}_2$ with **2-Cl** at $-20\text{ }^\circ\text{C}$ in CD_2Cl_2 . The solvent is indicated with an asterisk and signals corresponding to residual *o*-xylene are indicated by blue circles.

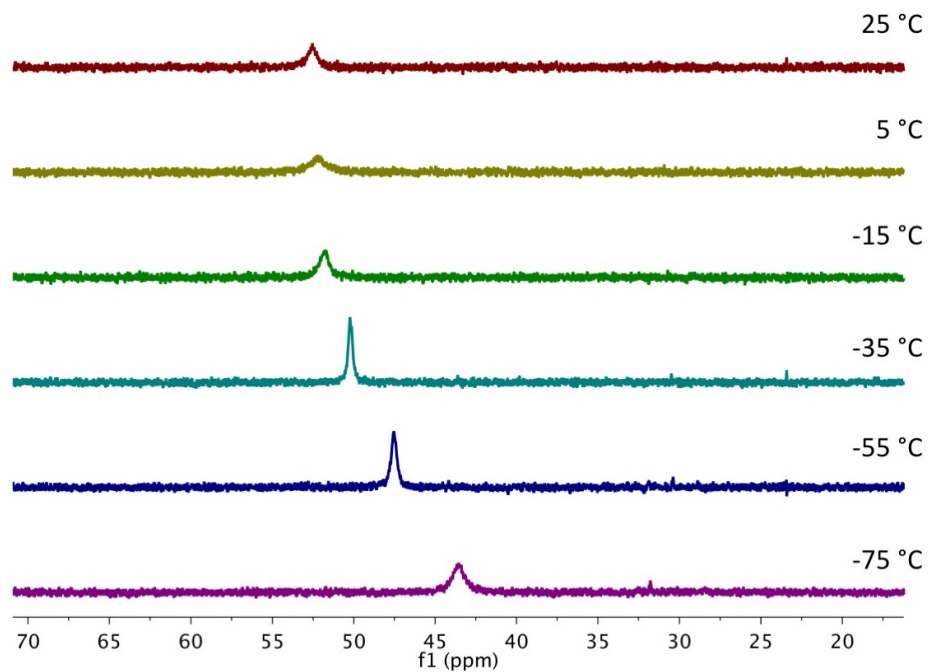


Figure S2. Variable temperature $^{31}\text{P}\{^1\text{H}\}$ NMR spectra (243 MHz) of 4-Cl.

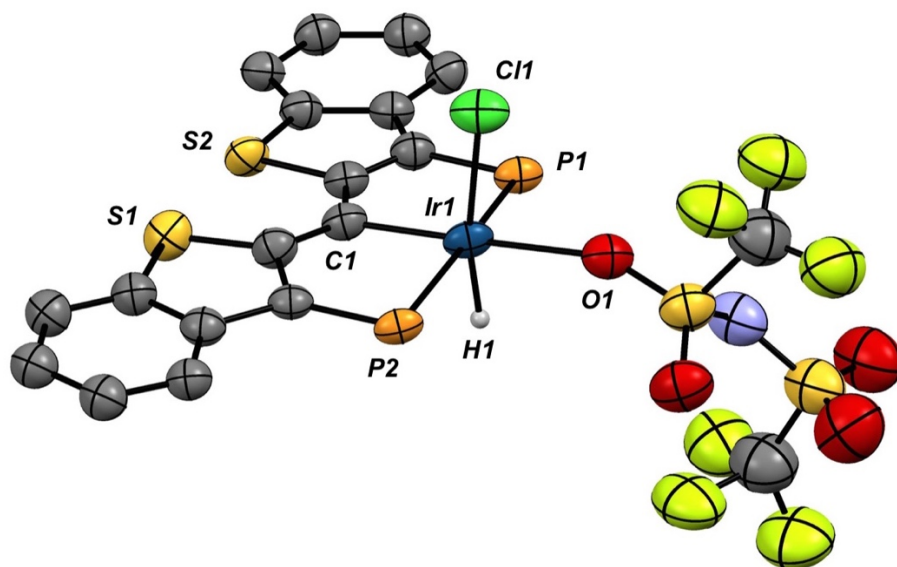


Figure S3. Molecular structure of 4-Cl. Hydrogen atoms except H1 have been omitted for clarity. Displacement ellipsoids are shown at the 50% probability level. Data collection for this structure is incomplete.

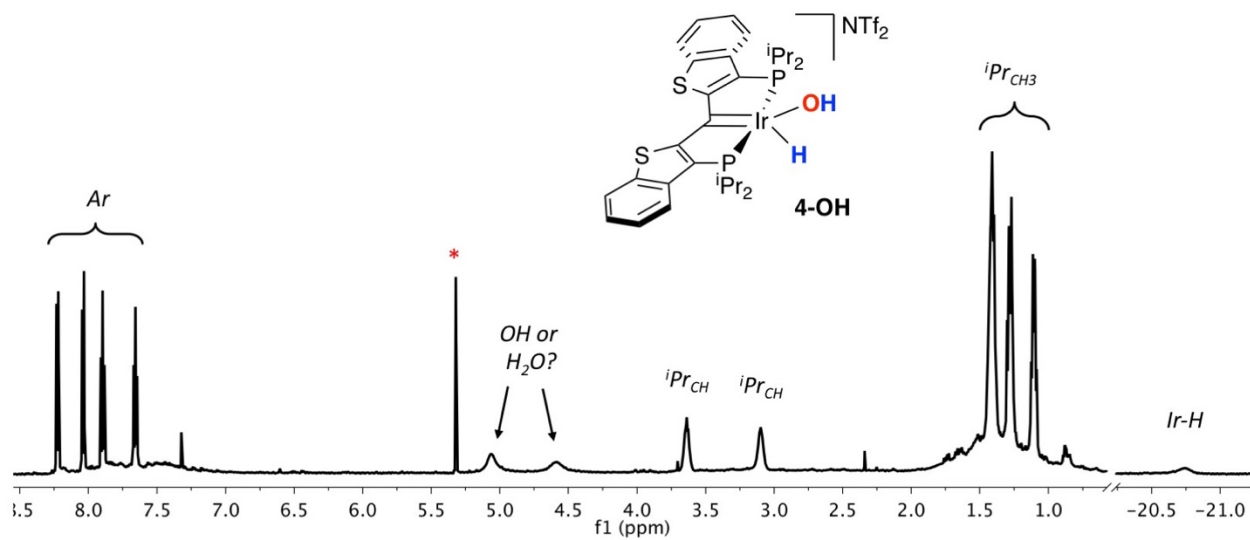


Figure S4. ^1H NMR spectrum of **4-OH** in CD_2Cl_2 (indicated with an asterisk).

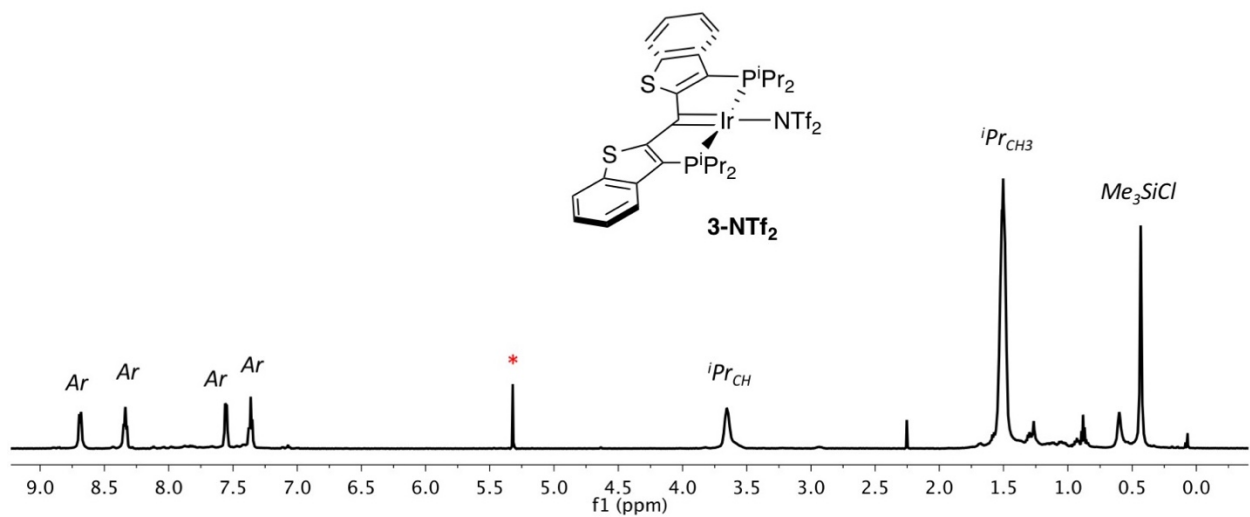


Figure S5. ^1H NMR spectrum of **3-NTf₂** in CD_2Cl_2 (indicated with an asterisk).

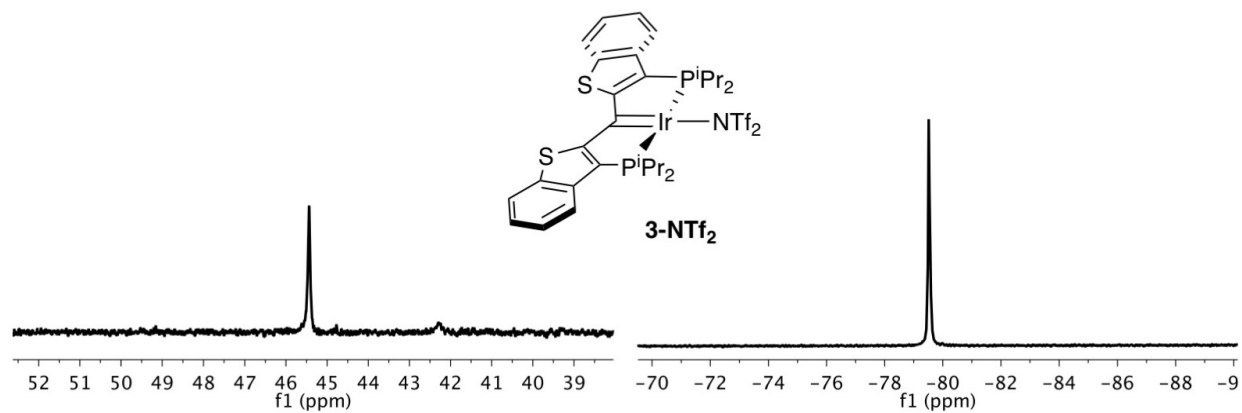


Figure S6. $^{31}\text{P}\{^1\text{H}\}$ (left) and ^{19}F (right) NMR spectra of **3-NTf₂** in CD_2Cl_2 .

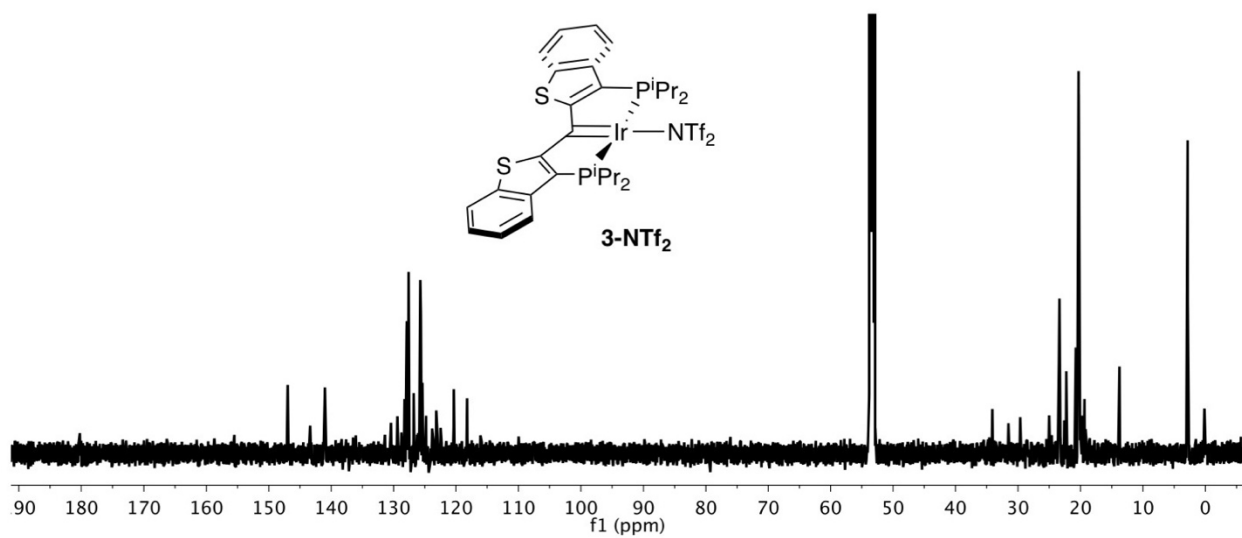


Figure S7. $^{13}\text{C}\{^1\text{H}\}$ NMR spectrum of **3-NTf₂** in CD_2Cl_2 .

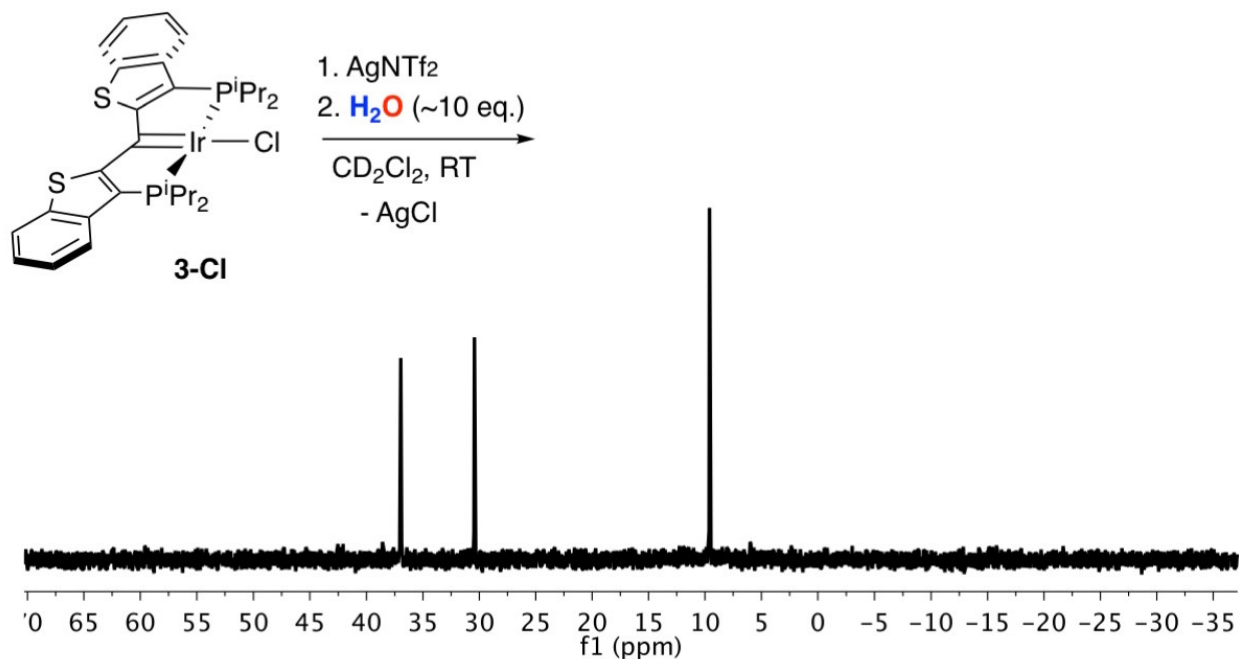


Figure S8. $^{31}\text{P}\{^1\text{H}\}$ NMR spectrum in CD_2Cl_2 of the reaction of **3-Cl**, AgNTf_2 and excess water.

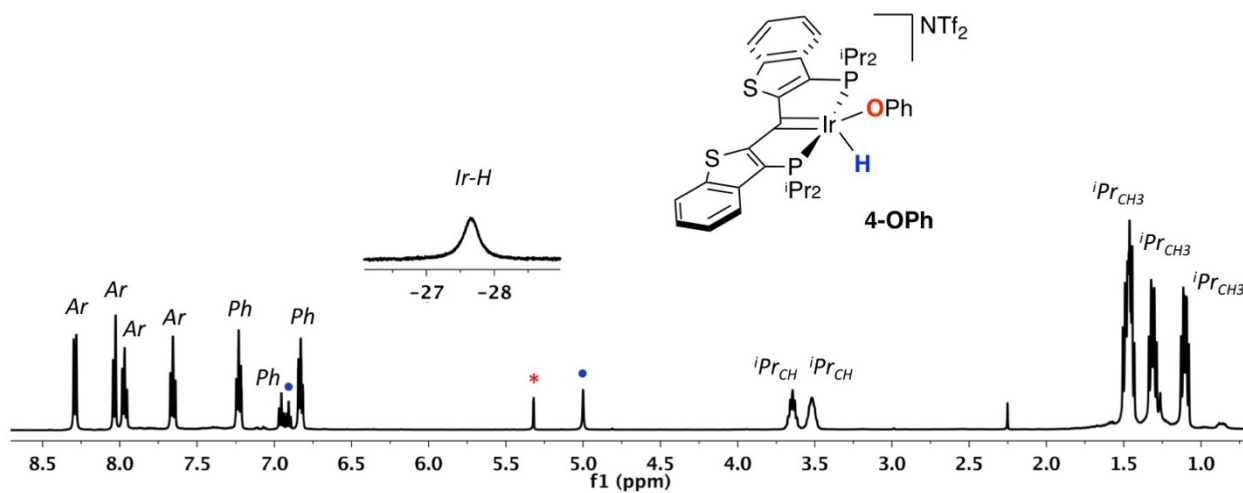


Figure S9. ^1H NMR spectrum of **4-OPh** in CD_2Cl_2 (indicated with an asterisk). Blue circles correspond to excess phenol.

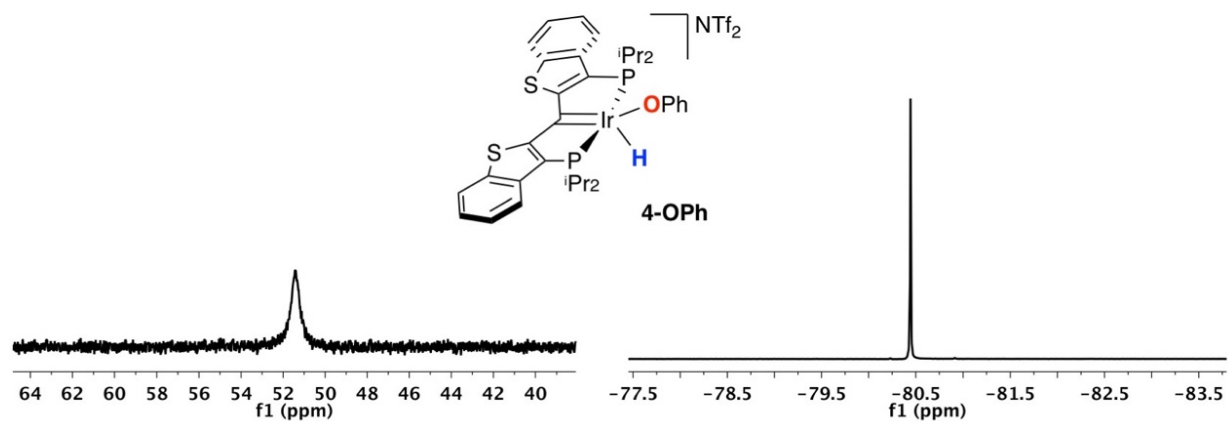


Figure S10. $^{31}\text{P}\{^1\text{H}\}$ (left) and ^{19}F (right) NMR spectra of **4-OPh** in CD_2Cl_2 .

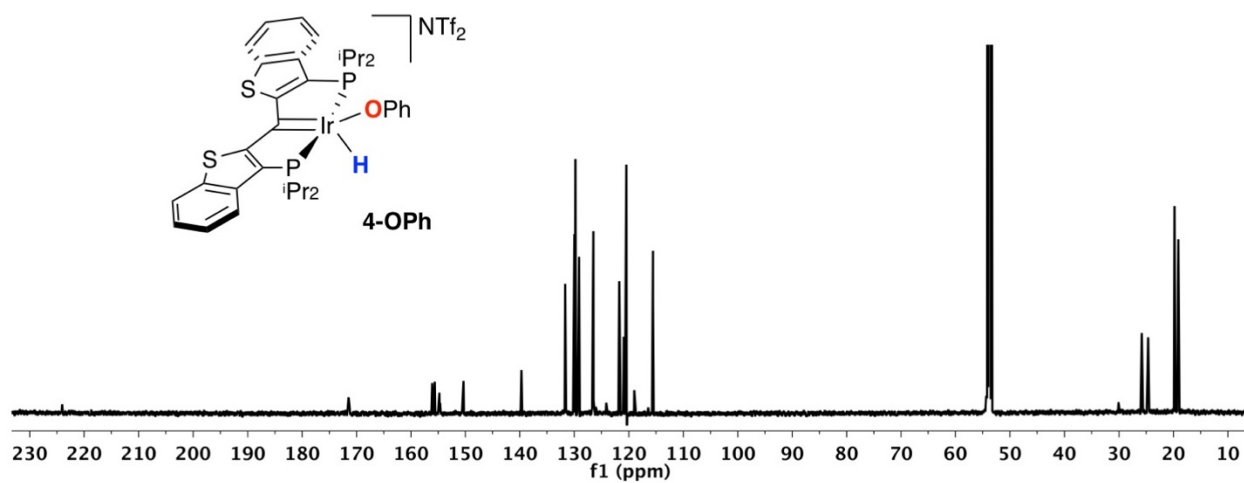


Figure S11. $^{13}\text{C}\{^1\text{H}\}$ NMR spectrum of **4-OPh** in CD_2Cl_2 .

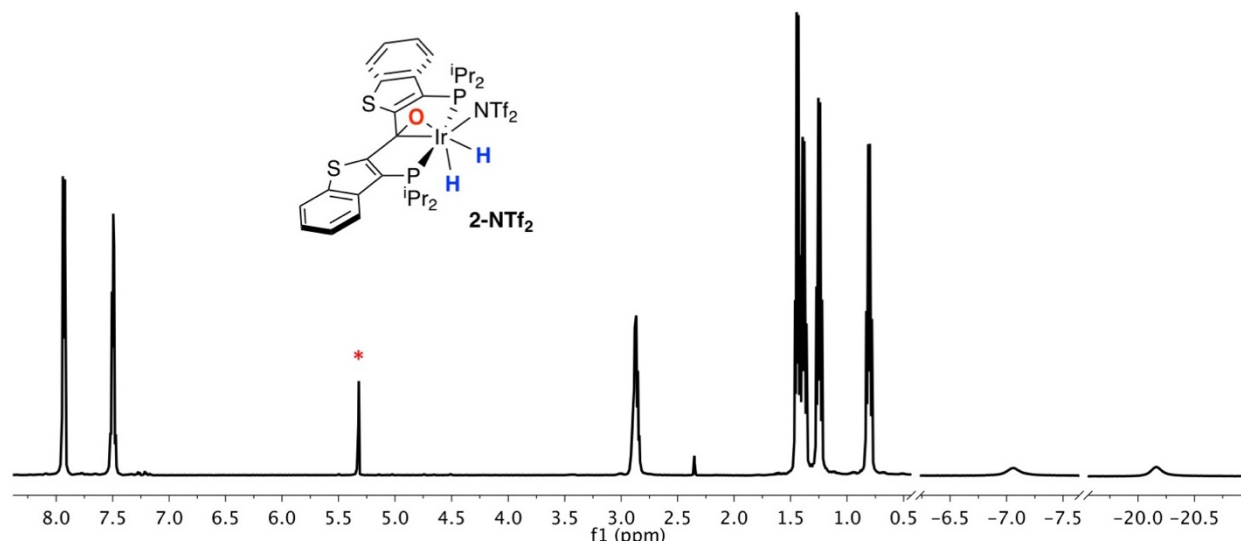


Figure S12. ^1H NMR spectrum of **2-NTf₂** in CD_2Cl_2 (indicated with an asterisk).

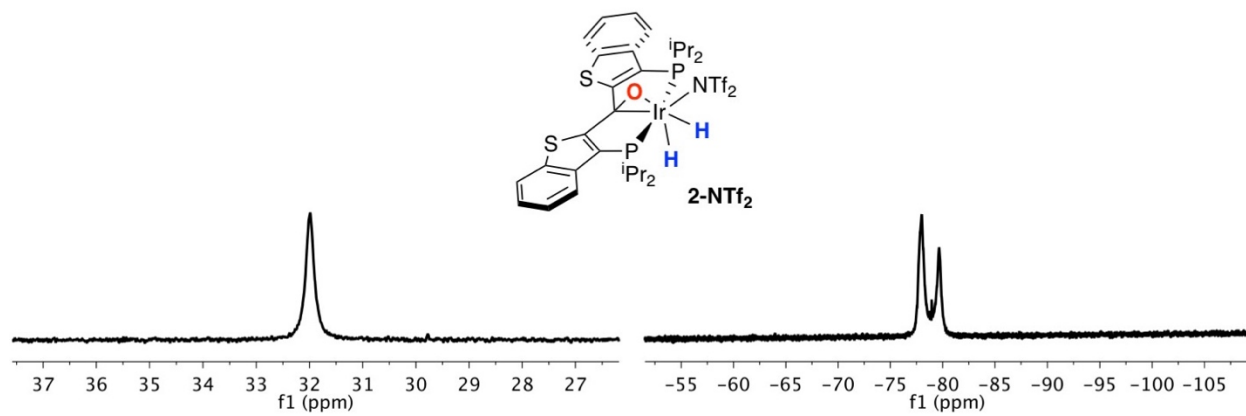


Figure S13. $^{31}\text{P}\{^1\text{H}\}$ (left) and ^{19}F (right) NMR spectra of **2-NTf₂** in CD_2Cl_2 .

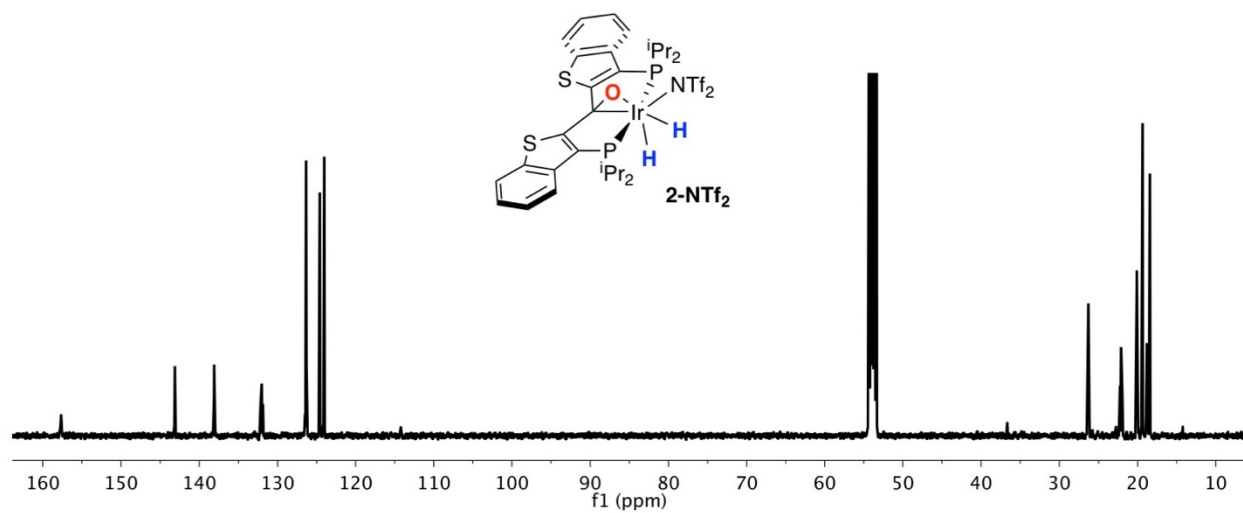


Figure S14. $^{13}\text{C}\{^1\text{H}\}$ NMR spectrum of **2-NTf₂** in CD_2Cl_2 .

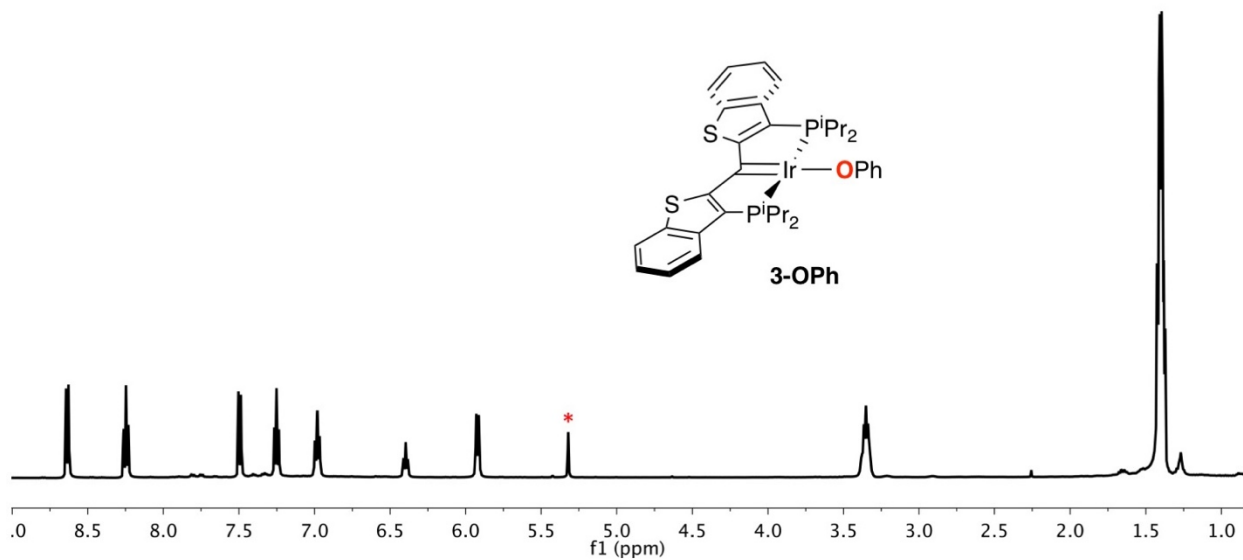


Figure S15. ^1H NMR spectrum of **3-OPh** in CD_2Cl_2 (indicated with an asterisk).

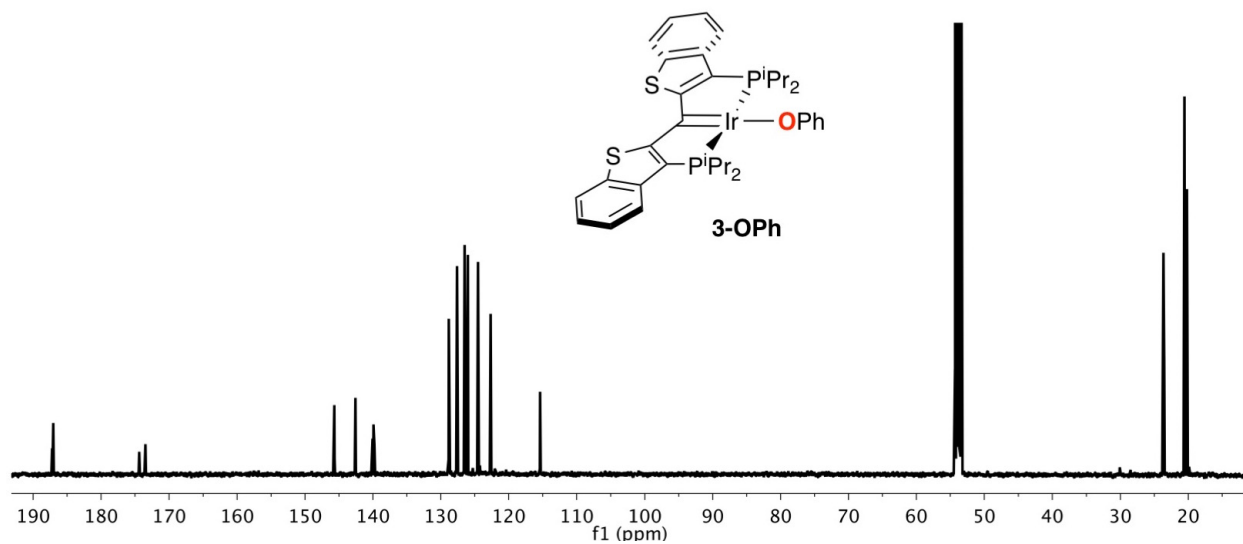


Figure S16. $^{13}\text{C}\{^1\text{H}\}$ NMR spectrum of **3-OPh** in CD_2Cl_2 .

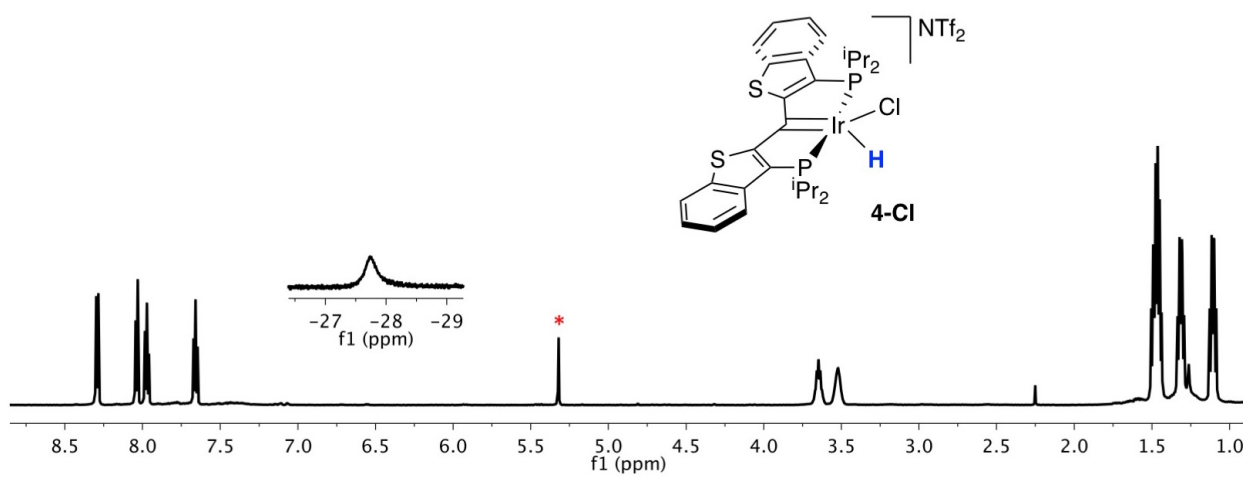


Figure S17. ^1H NMR spectrum of **4-Cl** in CD_2Cl_2 (indicated with an asterisk).

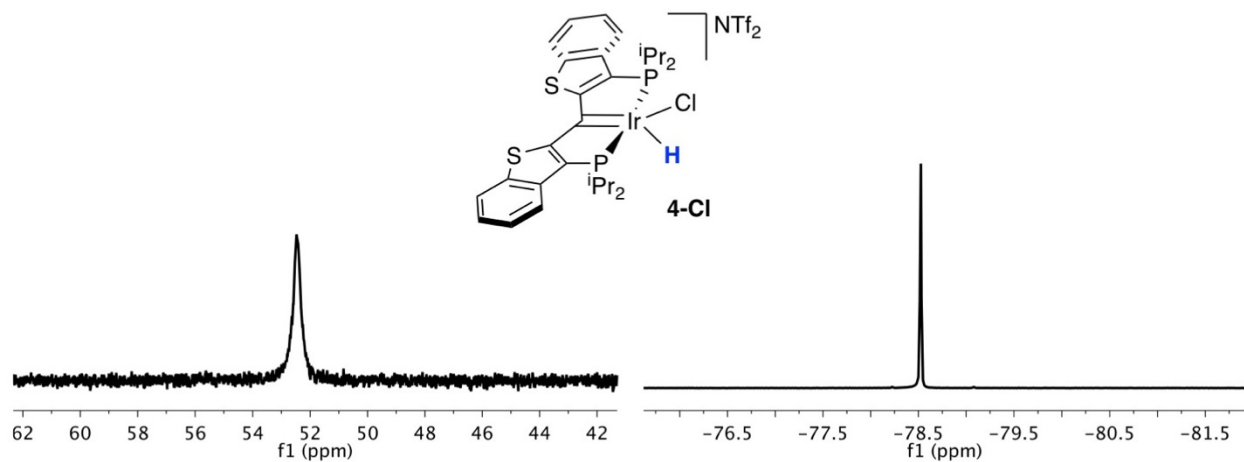


Figure S18. $^{31}\text{P}\{^1\text{H}\}$ (left) and ^{19}F (right) NMR spectra of **4-Cl** in CD_2Cl_2 .

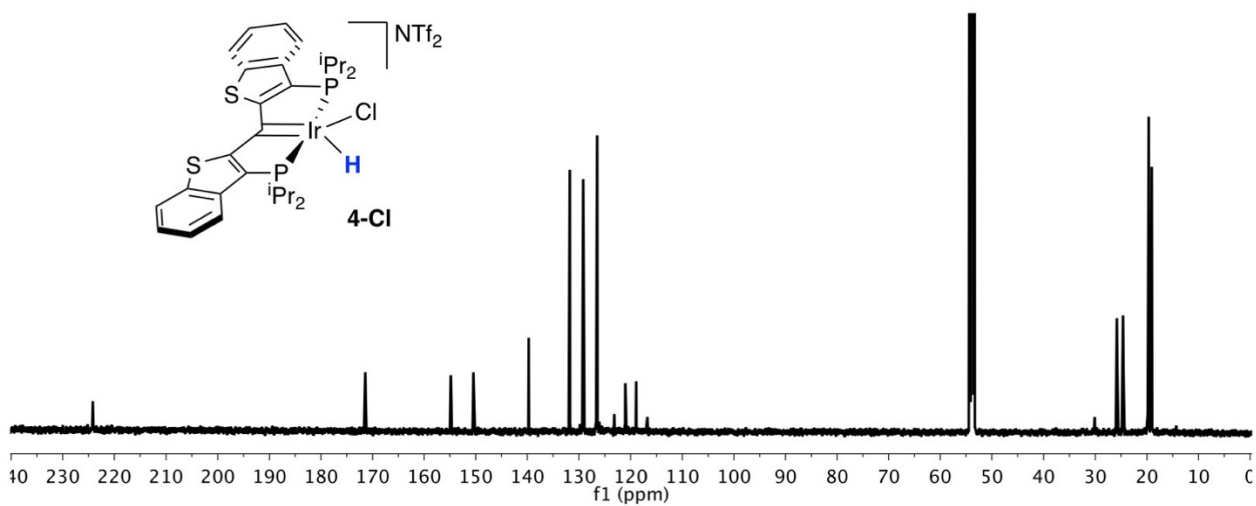


Figure S19. $^{13}\text{C}\{^1\text{H}\}$ NMR spectrum of **4-Cl** in CD_2Cl_2 .

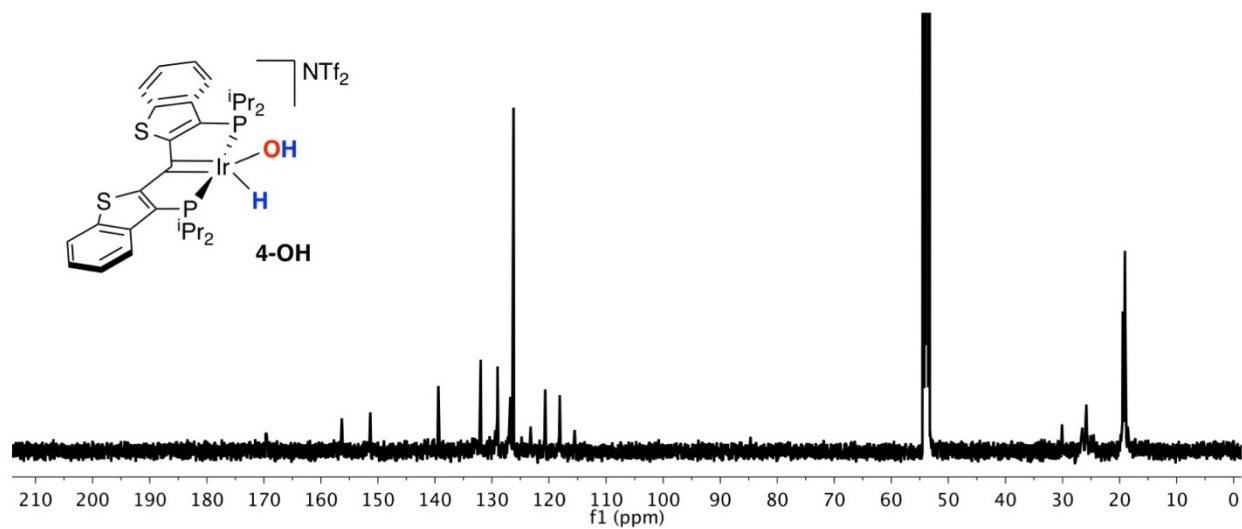


Figure S20. $^{13}\text{C}\{^1\text{H}\}$ NMR spectrum of **4-OH** in CD_2Cl_2 .

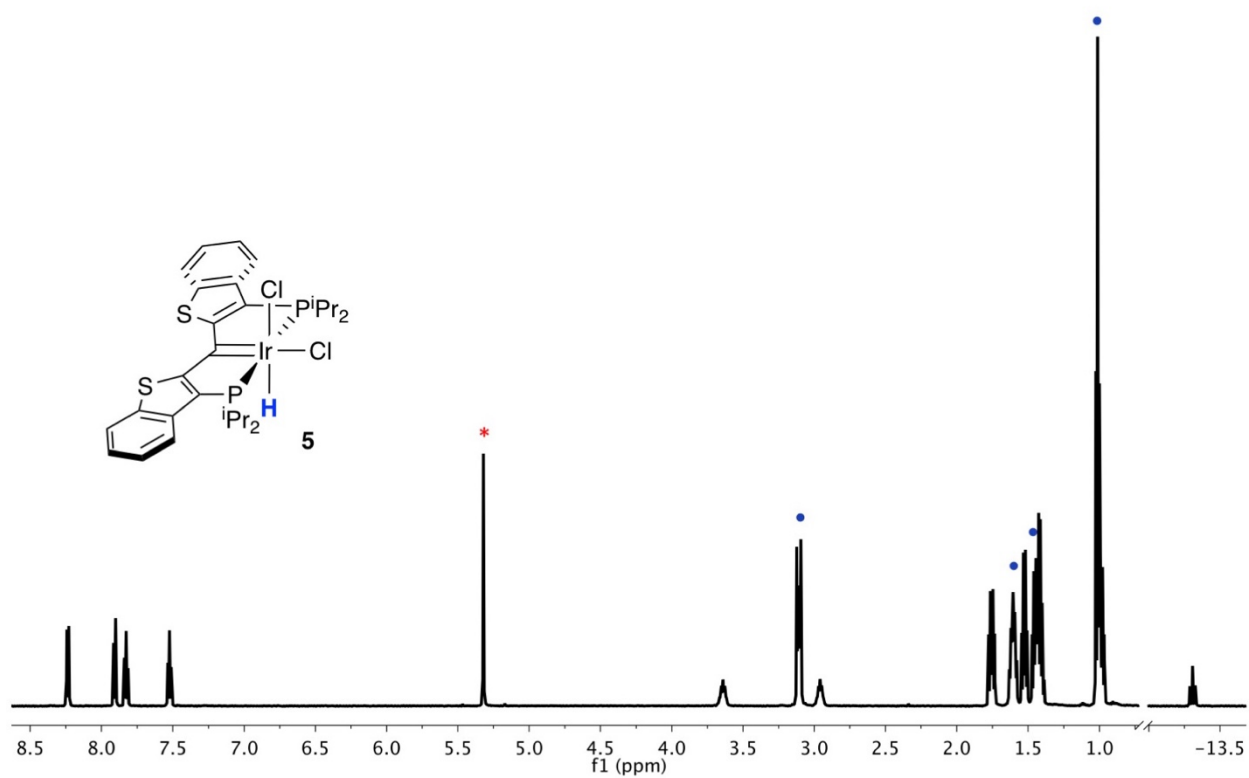


Figure S21. ^1H NMR spectrum of **5** in CD_2Cl_2 (indicated with an asterisk). Blue circles indicate the $n\text{Bu}_4\text{NNTf}_2$ byproduct.

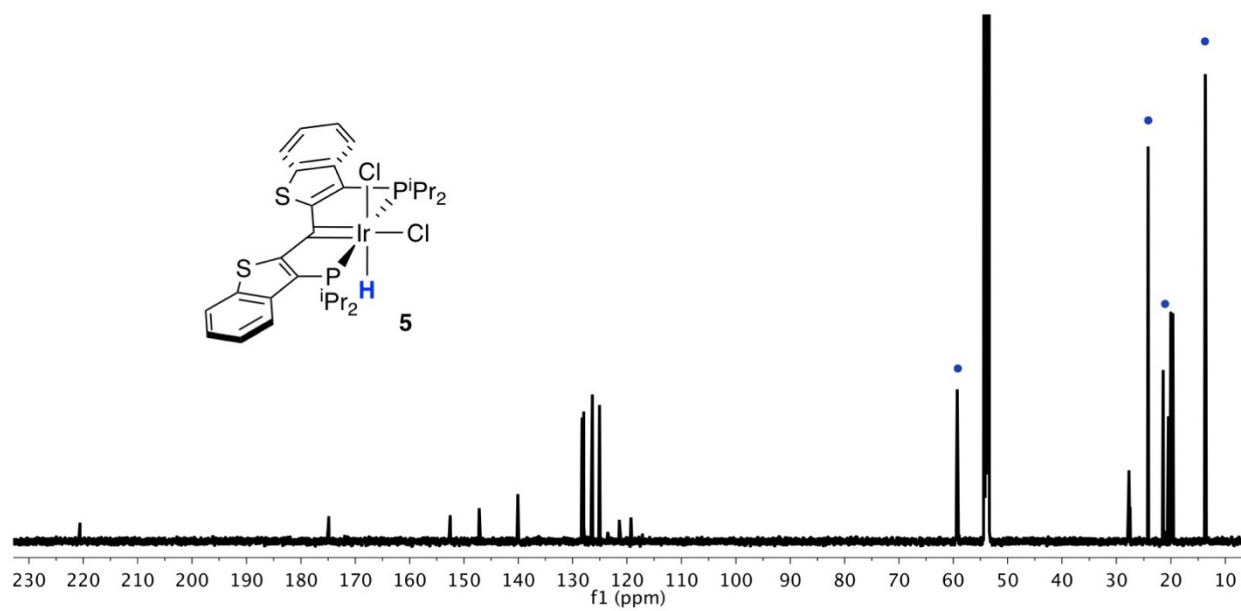


Figure S22. $^{13}\text{C}\{^1\text{H}\}$ NMR spectrum of **5** in CD_2Cl_2 . Blue circles indicate the $^n\text{Bu}_4\text{NNTf}_2$ byproduct.

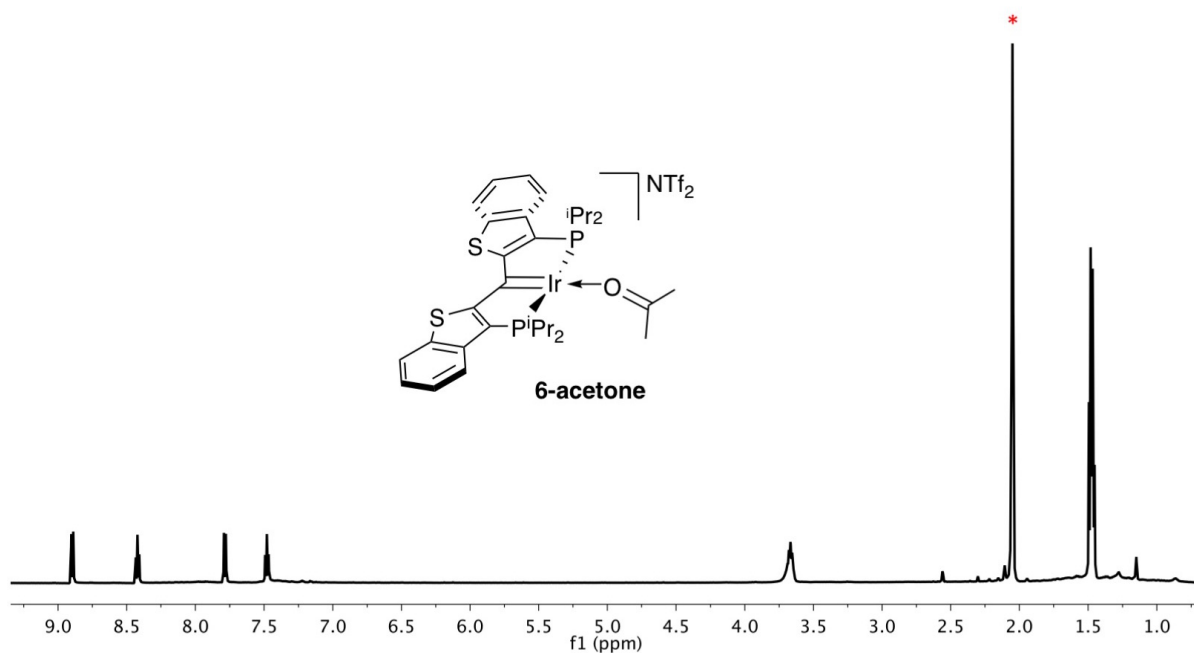


Figure S23. ^1H NMR spectrum of **6-acetone** in acetone- d_6 (indicated with an asterisk).

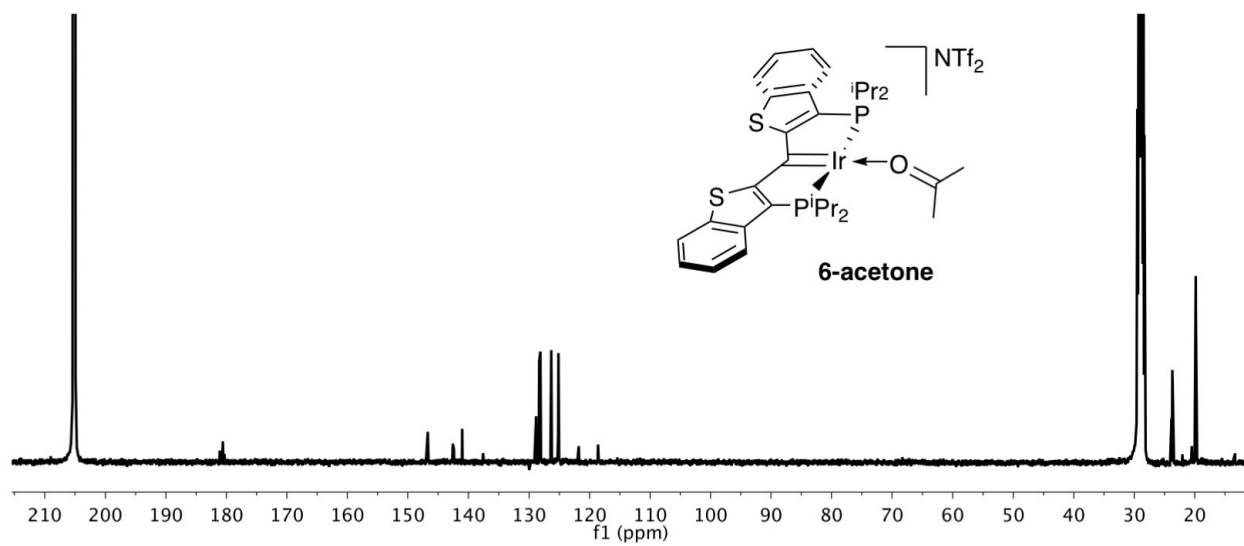


Figure S24. $^{13}\text{C}\{^1\text{H}\}$ NMR spectrum of **6-acetone** in $\text{acetone-}d_6$.

Table S1. Data collection and structure refinement details for **4-Cl**, **2-NTf₂** and **6-acetone**.

	4-Cl	2-NTf₂	6-acetone
formula	C ₃₁ H ₃₇ ClF ₆ IrNO ₄ P ₂ S ₄	C ₃₁ H ₃₈ F ₆ IrNO ₅ P ₂ S ₄	C ₃₂ H ₄₂ IrOP ₂ S ₂ , C ₂ F ₆ NO ₄ S ₂ , C ₃ H ₆ O
<i>fw</i>	1202.29	1001.00	1099.14
crystal system	Triclinic	Orthorhombic	Triclinic
space group	P -1	P b c a	P -1
<i>a</i> (Å)	11.448(2)	19.0520(3)	8.095(2)
<i>b</i> (Å)	14.330(3)	16.3670(8)	15.580(3)
<i>c</i> (Å)	23.826(5)	23.8210(4)	18.098(4)
<i>α</i> (deg)	104.190(4)	90	102.04(3)
<i>β</i> (deg)	94.070(4)	90	90.11(3)
<i>γ</i> (deg)	93.745(4)	90	92.16(3)
<i>V</i> (Å³)	3766.2(13)	7428.0(4)	2230.6(9)
<i>Z</i>	4	8	2
<i>T</i> (K)	173(2)	173(2)	173(2)
Wavelength (Å)	1.54178	0.7107	0.7107
ρ_{calcd} (g·cm⁻³)	2.120	1.790	1.636
<i>F</i>(000)	2360	3968	1100
μ (mm⁻¹)	9.966	3.976	3.320
crystal size, mm³	0.05×0.05×0.001	0.720×0.560×0.420	0.280×0.260×0.220
transmission factors	? – ?	0.088 – 0.166	0.416 – 0.478
<i>θ</i> range (deg)	1.920 – 37.859	3.045 – 27.508	2.779 – 28.658
data/restraints/param	3746/1433/953	8514/154/467	11422/7/623
GOF	0.935	1.062	1.083
R₁ [<i>I</i> > 2σ(<i>I</i>)]	0.0491	0.0263	0.0322
wR₂ [all data]	0.1719	0.0609	0.0699
residual density, e/Å³	0.910 and -0.654	0.713 and -0.911	1.036 and -0.622